Global Journal of Engineering and Technology Advances
eISSN: 2582-5003
Cross Ref DOI: 10.30574/gjeta
Journal homepage: https://gjeta.com/

(REVIEW ARTICLE)

Check for updates

A comparative study of voltage stability NVSI Index and load margin index

Zhikui Zhang *, Yuan Gao and Xin Wang

School of Electric Power Engineering, Nanjing Institute of Technology, Nanjing, Jiangsu, China.

Global Journal of Engineering and Technology Advances, 2023, 17(01), 094–103

Publication history: Received on 02 September 2023; revised on 08 October 2023; accepted on 11 October 2023

Article DOI: https://doi.org/10.30574/gjeta.2023.17.1.0209

Abstract

With the development of new energy generation technologies, photovoltaic (PV) power generation has gained widespread application as a clean and sustainable source of electricity. However, the intermittency and variability of PV generation pose new challenges to power system secure and stable operation. The WSCC 9-bus system is used in this paper to investigate the effect of PV integration on static voltage stability in power systems. An improved voltage stability index (NVSI) considering the new energy was used to measure the voltage stability of the access point of PV plant. Compared with the *P-V* curve and the classic load margin index (I_{LM}), even if the index value is less than 0, the NVSI index has still a better measure effect on voltage stability.

Keywords: Voltage stability; Photovoltaic generation; *P-V* curve; NVSI index; Load margin index

1. Introduction

With the continuous growth in energy demand and the increasing prominence of environmental issues, ongoing research and utilization of renewable energy technologies have become crucial steps towards replacing fossil fuels and achieving green and sustainable development. Among these technologies, photovoltaic (PV) generation has emerged as a focal point in the transition towards clean energy due to its characteristics of being pollution-free, renewable, and having a wide distribution of energy sources. From 2021 to 2026, the annual average increment of global renewable power capacity is expected to reach approximately 305GW, with a growth rate of nearly 60% (IEA, 2021). According to the International Energy Agency statistics, by the year 2050, global net electricity generation from solar energy is projected to exceed 100,000 terawatt-hours (EIA, 2021)[1].

However, the introduction and grid integration of PV systems have given rise to a series of power system stability issues, with voltage stability being one of the increasingly prominent concerns [2-3]. Voltage instability is often triggered by load-related factors, occurring when the load exceeds the generation capacity of the interconnected power grid. As the share of renewable energy generation increases, owing to the stochastic and uncertain nature of renewable generation and the rising levels of daily electricity consumption, the static voltage stability margin of today power systems has decreased [4]. Research [5] has demonstrated that PV power systems can help address overvoltage issues in the power system by absorbing reactive power. In order to enhance the monitoring of voltage conditions in the power system, scientists have been exploring various voltage stability indexes to identify the weakest lines and buses [6]. A voltage stability index, L_{mn}, is introduced in Reference [7] to assess the stability of connection lines between two buses. The improved voltage index (IVSI), which is based on power flow calculations, is shown in reference [8]. The study cited in reference [9] takes into account the impact of integrating renewable energy sources such as wind and PV and proposes an improved voltage stability index, NVSI.

This paper primarily investigates the impact of grid-connected PV systems on the static voltage stability of the power system. It utilizes the voltage stability index mentioned in reference [9] to assess system bus voltage stability and

* Corresponding author: Zhikui Zhang

suggest improvements. This paper uses the WSCC 9-bus system to simulate the validation of the impact of the grid-connected PV system on the voltage stability by comparing the pre- and post-incorporated PV.

2. Analysis Techniques

2.1. Voltage stability index

Voltage stability index is used to identify buses with weaker voltage stability within the power system. During regular power system operation, each load bus situation is judged by index. Each load bus index value falls between 0 and 1, with values closer to 1 indicating poorer voltage stability, suggesting more robust voltage stability for values closer to 0. The NVSI mentioned in reference [9] is an improvement over the IVSI introduced in reference [8]. NVSI considers the impact of newly injected renewable energy sources in the system, making it more applicable to modern power systems. The formula of *NVSIi* for each bus is as shown in formula (1):

$$NVSI_i = \frac{-4\sum_{j=0}^{n}(G_{ij} - B_{ij})(P_i + P_{new} + Q_i + Q_{new})}{\{\sum_{j=1}^{n} V_j[(G_{ij} - B_{ij})\cos\delta_{ij} + (G_{ij} + B_{ij})\sin\delta_{ij}]\}^2} \quad \text{.....(1)}$$

Where V_j represents the voltage of the terminal bus, δ_{ij} represents a voltage angle between bus *i* and bus *j*; G_{ij}, B_{ij} indicates the conductance and susceptance on the line between bus *i* and bus *j*, which can be obtained in the nodal conductor matrix; P_i and Q_i indicate the active power and reactive power injected by the grid into the bus *i* ; P_{new} and Q_{new} denote the active and reactive power injected by the photovoltaic system at bus *i.*

When the injection power of the new energy on the bus is zero (P_{new}= Q_{new}=0), the NVSI expression is equal to the IVSI expression. The formula for $IVSI_i$ is as follows (2):

$$IVSI_i = \frac{-4\sum_{j=0}^{n}(G_{ij} - B_{ij})(P_i + Q_i)}{\{\sum_{j=1}^{n} V_j[(G_{ij} - B_{ij})\cos\delta_{ij} + (G_{ij} + B_{ij})\sin\delta_{ij}]\}^2} \quad \text{.....(2)}$$

2.2. *P-V* curve

The *P-V* curve is a commonly used method in power system analysis for assessing voltage stability. The bus voltage is obtained by incrementally increasing the power demand on the bus. Eventually, this process forms a characteristic nose-shaped curve, where the "nose" of the curve represents the critical point at which voltage collapse occurs. When the voltage at a bus drops below a critical level, it results in voltage collapse, which is marked by a sustained decrease in voltage levels.

Constructing a *P-V* curve involves using Continuous Power Flow (CPF) calculations. This approach is chosen because the Jacobian matrix becomes singular near the critical point, causing conventional power flow calculations to become challenging to continue. Consequently, CPF has been investigated to compensate for this deficiency. The process of CPF calculations typically adheres to a prediction-correction scheme, as outlined in references [10-12]:

$$(x^j, \lambda^j) \xrightarrow{\text{predictor}} (\hat{x}^{j+1}, \hat{\lambda}^{j+1}) \xrightarrow{\text{corrector}} (x^{j+1}, \lambda^{j+1}) \quad \text{.....(3)}$$

where (x^j,λ^j) is the initial solution, ($\hat{x}^{j+1}$,$\hat{\lambda}^{j+1}$) is the predicted solution and (x^{j+1},λ^{j+1}) is the corrected solution.

The calculation methodology for CPF entails the selection of a new continuous parameter, followed by predicting power flow solutions at that parameter value. Typically, the chosen parameter is either voltage or power. The power flow equations are the following formulation:

$$F(\delta, v, \lambda) = g(\delta, v) - K\lambda = 0 \quad \text{.....(4)}$$

In formula (4), $g(\delta, v)$ represents the standard power flow calculation equation, where K signifies the distribution characteristics of variable loads, and λ denotes the load parameter. Because there is an extra variable in the equation, a linear equation is added to solve the CPF:

$$\begin{bmatrix} \frac{\partial f}{\partial \delta}, \frac{\partial f}{\partial v}, \frac{\partial f}{\partial \lambda} \\ e^k \end{bmatrix} \begin{bmatrix} d\delta \\ dv \\ d\lambda \end{bmatrix} = \begin{bmatrix} 0 \\ 0 \\ 1 \end{bmatrix} \text{.....(5)}$$

The vector e^k is defined such that all members, except for the selected parameter being either 1 or -1, are assigned a value of 0.

The parameters are predicted using the following methodology:

$$\begin{bmatrix} \delta \\ v \\ \lambda \end{bmatrix}^{\text{pre}} = \begin{bmatrix} \delta_0 \\ v_0 \\ \lambda_0 \end{bmatrix} + \sigma \begin{bmatrix} d\delta \\ dv \\ d\lambda \end{bmatrix} \text{.....(6)}$$

Where $(\delta_0, v_0, \lambda_0)$ represents the solution of equation (5), σ denotes the predicted step size. Let $x_k = [\delta, v, \lambda]$.

The equation set for the correction step is as follows:

$$\begin{cases} F(\delta, v, \lambda) = 0 \\ x_k - x_k^{\text{pre}} = 0 \end{cases} \text{.....(7)}$$

$$\sigma_{\min} < \sigma < \sigma_{\max} \text{.....(8)}$$

The correction step uses the equation (7) to obtain the corrected values, which are then used for iterative calculations. Inequality (8) is the criterion for determining whether to continue with the iterative calculations. If the inequality is satisfied, the iterations continue; otherwise, the computation is terminated.

Based on the above CPF calculations, plot the relationship curve between the load parameter λ and bus voltage V on a coordinate axis to obtain the *P-V* curve. The illustration of this concept is presented in Figure 1 as follows:

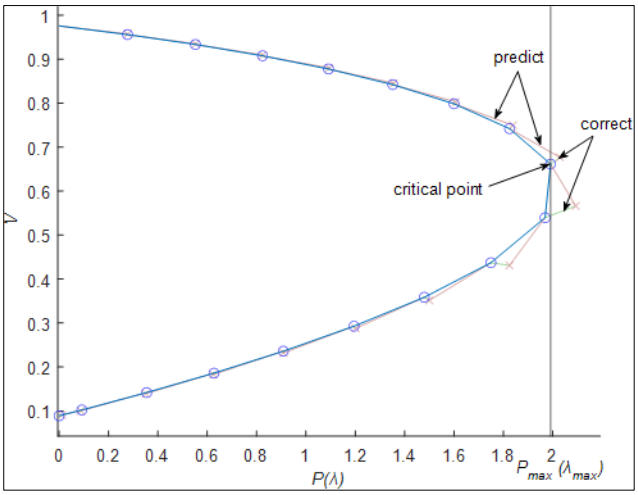

Figure 1 *P-V* curve

2.3. Load margin index

The load margin index at that bus can be computed after getting the *P-V* curve. The load margin index measures the voltage stability of the system by quantifying the distance between the current load power and the load power at the voltage stability critical point. The formula for calculating the load margin index is as follows [13,14]:

$$I_{\mathrm{LM}} = \frac{P_{\mathrm{MAX}} - P}{P_{\mathrm{MAX}}} \quad \text{.....(9)}$$

In Equation (9), P_{MAX} is the load at the *P-V* curve critical point for the bus, and *P* is the load active power of the bus in the current system to be determined. Since the *P-V* curve is derived using the CPF, its abscissa is represented by λ. The expression is as follows:

$$\lambda = \frac{P}{P_0} \quad \text{.....(10)}$$

$$\lambda_{\mathrm{MAX}} = \frac{P_{\mathrm{MAX}}}{P_0} \quad \text{.....(11)}$$

P_0 represents the active power load at the bus in the initial operating state of the system. Substituting equation (10) into equation (9) yields:

$$I_{\mathrm{LM}} = 1 - \frac{\lambda}{\lambda_{\mathrm{MAX}}} \quad \text{.....(12)}$$

In CPF, the current system operating state is identical to the initial operating state, i.e., P_0=*P*, and thus λ = 1 per unit (pu), the ultimate expression for the load margin index is as follows:

$$I_{\mathrm{LM}} = 1 - \frac{1}{\lambda_{\mathrm{MAX}}} \quad \text{.....(13)}$$

The closer the value of I_{LM} is to 1, the better the voltage stability of the system. Conversely, the closer it is to 0, the weaker the voltage stability of the system.

3. Simulation and result analysis

3.1. WSCC 9-bus system

Figure 2 shows the WSCC 9-bus system. Bus 1 is the slack bus, bus 2 and 3 are PV buses. Bus 5, 6, and 8 represent load buses. In this system design, the total generator capacity is 519.5 MVA, and the total load is 315 + j115 MVA.

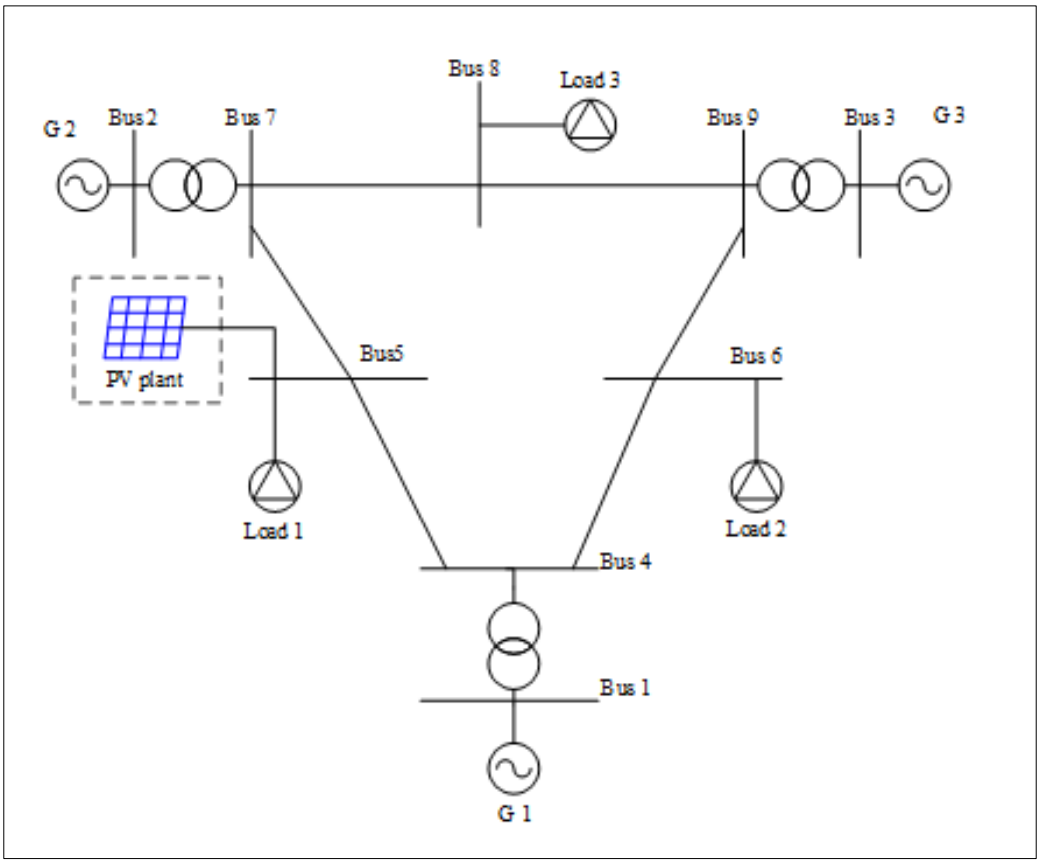

Figure 2 WSCC 9-bus system

3.2. Calculation of indexes for load buses

Voltage collapse typically starts from the bus with the weakest voltage stability in the power system, ultimately leading to a system-wide breakdown. Therefore, identifying the bus with the weakest voltage stability in the system is of utmost importance. The calculation of IVSI and I_{LM} for each load bus is performed using equation (2) and equation (13), and the corresponding outcomes are presented in Table 1. Concurrently, *P-V* curves for bus 5, 6, and 8 were plotted, as illustrated in Figure 3:

Table 1 The values of IVSI and I_{LM} for load buses

	Bus5	**Bus6**	**Bus8**
IVSI	0.303976	0.220839	0.16399
I_{LM}	0.69356	0.76988	0.8118

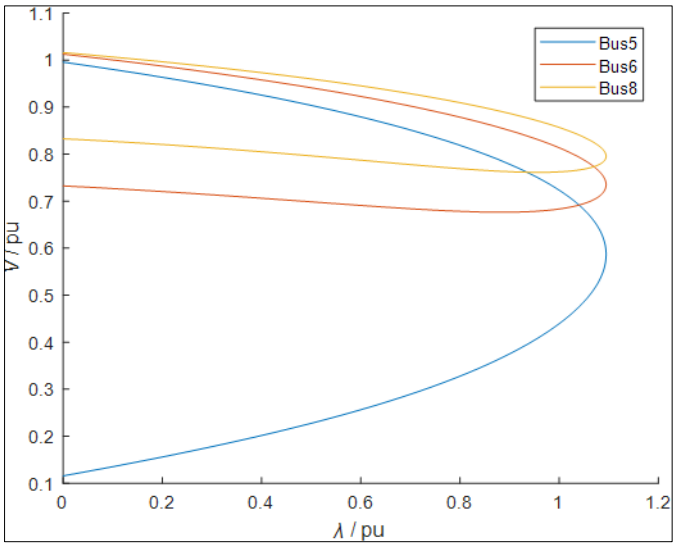

Figure 3 *P-V* curve of load buses

The total load in the system is increased by a factor of x (x = 1.1, 1.2, ... 2.5) of the initial value, and the change in the IVSI and I_{LM} values of the three load buses in the system is observed. As shown in Table 2:

Table 2 IVSI and I_{LM} index values for load buses after load change

***x* Base load**	**Bus5**		**Bus6**		**Bus8**	
	IVSI	**I_{LM}**	**IVSI**	**I_{LM}**	**IVSI**	**I_{LM}**
1.1	0.3327	0.6330	0.2425	0.7292	0.1805	0.7806
1.3	0.3904	0.5693	0.2864	0.6848	0.2137	0.7465
1.5	0.4492	0.5005	0.3317	0.6366	0.2475	0.7102
1.7	0.5103	0.4249	0.3795	0.5827	0.2823	0.6714
1.9	0.5755	0.3376	0.4313	0.5202	0.3185	0.6292
2.1	0.6484	0.2288	0.4903	0.4401	0.3570	0.5808
2.3	0.7385	0.0744	0.5648	0.2995	0.4005	0.5103
2.5	1.0348		0.8568		0.4969	

From Figure 4(a), it can be seen that the IVSI values of the load buses in the system increase as the load increases. When the load reaches 2.5 times its initial value, the IVSI value for bus 5 exceeds 1, indicating that voltage collapse has occurred. In Figure 4(b), the I_{LM} values decrease as the system load increases. When the system load increases by a factor of 2.5, the CPF calculation no longer converges, rendering the I_{LM} value non-existent. The figure above illustrates that the rate of IVSI increase at bus 5 is the fastest, and its I_{LM} index decay rate is also the swiftest.

In summary, based on the comparison of IVSI, I_{LM}, and *P-V* curve results under various conditions, it is evident that bus 5 is the weakest bus. As the load on the bus increases, both IVSI and I_{LM} are effective in accurately assessing the static voltage stability of the system.

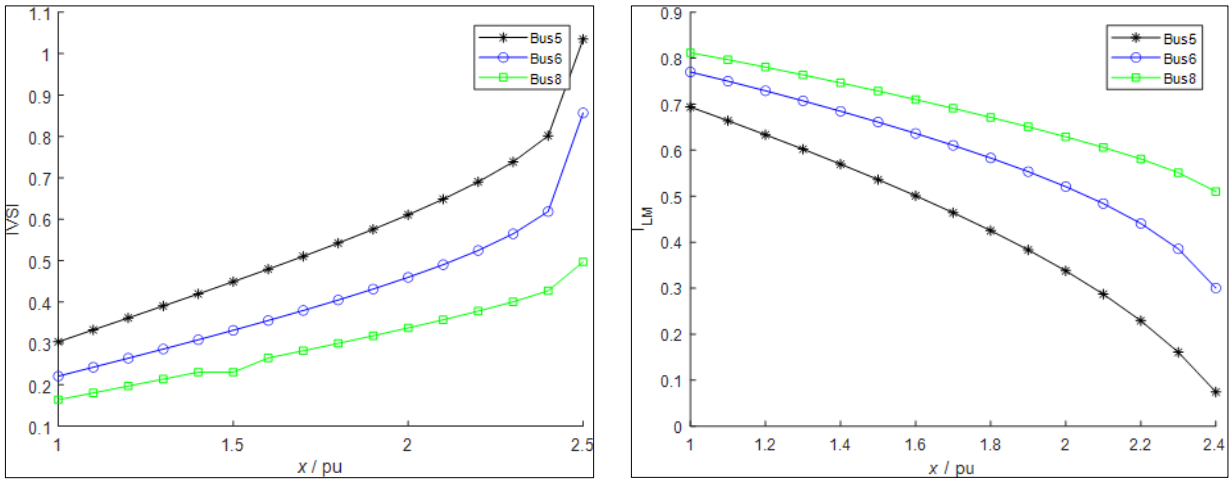

a **b**

Figure 4 IVSI and I_{LM} index of load buses after load change

3.3. Effect of PV plant

Based on the preceding analysis, there is a higher risk of voltage collapse at bus 5 within the system. Consequently, a decision has been made to integrate a PV plant with a capacity of 50 MW at bus 5. After integrating the PV plant, the NVSI and I_{LM} values for bus 5 are shown in Table 3.

Table 3 NVSI and I_{LM} values for bus 5 before / after adding PV

	Base case	**with PV plant**
NVSI	0.303976	0.22484
I_{LM}	0.69356	0.7168

Based on the data in the table, integrating PV plant at bus 5 decreased the NVSI index value and increased the load margin index value. This indicates that the integration of PV has improved the voltage stability at bus 5. The *P-V* curve for bus 5 after the integration of the PV is shown in Figure 5.

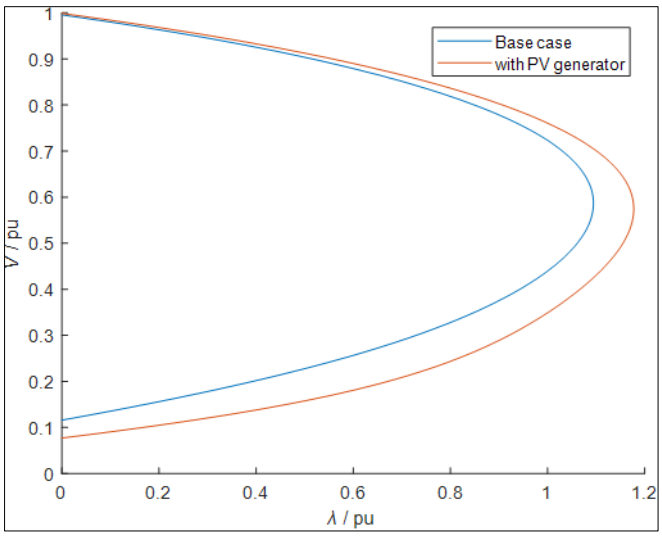

Figure 5 *P-V* curve for bus 5 before / after adding PV

The curve in Figure 5 shows that the voltage critical point at bus 5 with the PV has moved to the right. This shift indicates that the voltage drop at bus 5 alleviates as the load increases and the system load margin increases. The voltage stability of this bus has improved.

Load fluctuations in a power system are inherently uncontrollable. The magnitude of load increments at each load bus is also stochastic. To assess the impact of PV integration, we focused on observing changes in the NVSI and I_{LM} indexes at bus 5 before and after the addition of the PV plant. The calculations found that the bus voltage reached the critical point when the load at bus 5 increased to 3.254 times its initial value. After the PV integration, the bus voltage reached the critical point when the load at bus 5 increased to 3.5305 times its original value. As seen in Figure 6.

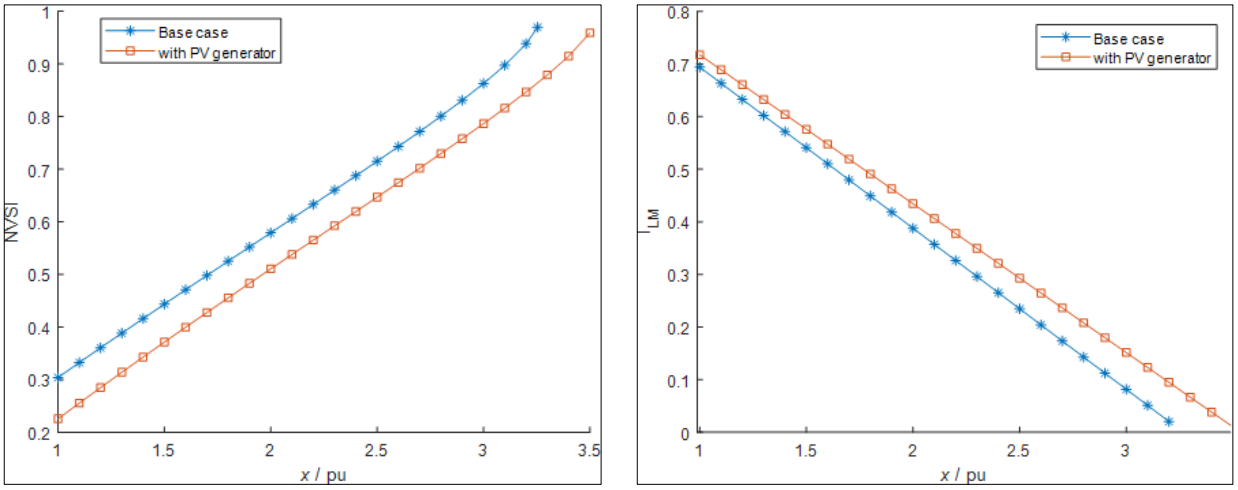

a b

Figure 6 Bus 5 indexes with load increase

In Figure 6(a), under the same load multiplier, the NVSI index value at bus 5 in the system before PV integration is more excellent than after integration. Under a load multiplier of 3.254, the NVSI index value at bus 5 in the original system is already very close to 1, while in the system with PV integration, the NVSI value at bus 5 is below 1. Figure 6(b) demonstrates that the integration of PV has expanded the load margin of the system, increasing the load limit from its original value of 3.254 times to 3.5305 times.

3.4. Effect of PV penetration

Due to its environmentally benign and sustainable nature, there is a growing desire to replace fossil fuel-based power generation with clean energy alternatives. The penetration level of renewable energy is a crucial factor influencing the static voltage stability of the power system. The PV penetration level depends on the system total generation capacity or total load demand.

Table 4 NVSI and I_{LM} values for bus 5 with various PV penetration

x **Base load**	**0% PV penetration**		**20% PV penetration**		**40% PV penetration**		**60% PV penetration**	
	NVSI	**I_{LM}**	**NVSI**	**I_{LM}**	**NVSI**	**I_{LM}**	**NVSI**	**I_{LM}**
1.0	0.3040	0.6936	0.1844	0.7272	-0.052	0.7679	-0.9125	0.8165
1.5	0.3957	0.5408	0.2849	0.5910	0.0733	0.6518	-0.6015	0.7245
2.0	0.4828	0.3873	0.3778	0.4546	0.1844	0.5359	-0.3760	0.6328
2.5	0.5676	0.2341	0.4656	0.3182	0.2849	0.4198	-0.1989	0.5415
3.0	0.6531	0.0817	0.5507	0.1810	0.3778	0.3036	-0.0524	0.4500

In Table 4, some NVSI values are negative. According to Equation (1), when the PV plant injected at a bus exceeds the load power at that bus, the NVSI value becomes negative. At the PV penetration level of 60% and load multipliers of 1.0

and 1.5, the NVSI value approaches -1, while the I_{LM} value approaches 1. Beyond the PV penetration level of 60%, the power flow calculations in the system no longer converge.

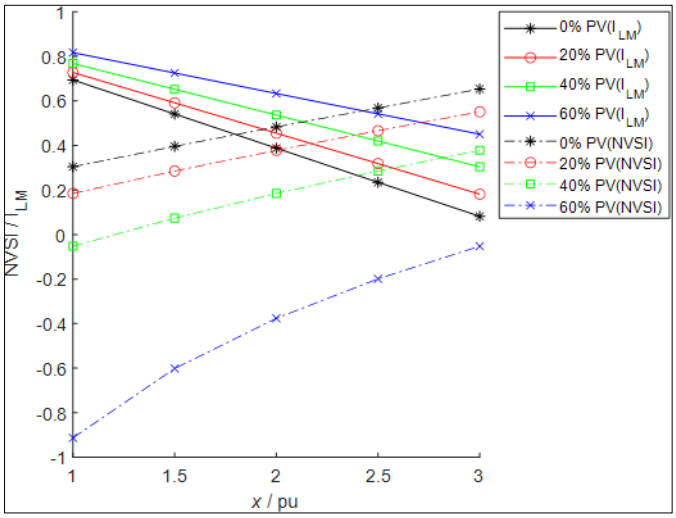

Figure 7 NVSI and I_{LM} with various PV penetration

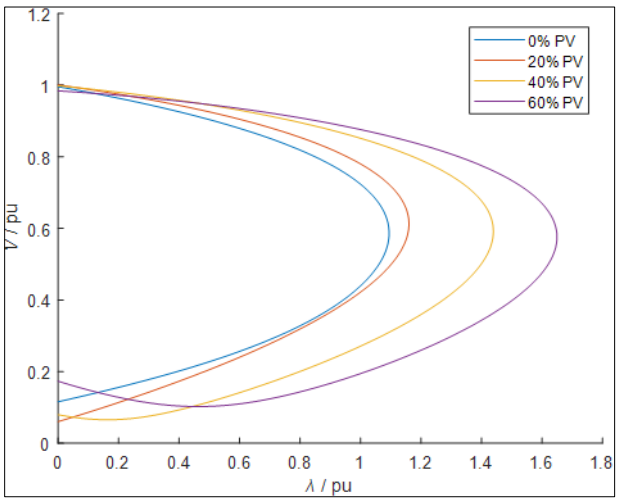

Figure 8 *P-V* curve with various PV penetration

Based on Figure 7, it is evident that at the 60% PV penetration level, all NVSI values are negative. When the load increases, the I_{LM} value goes down and the NVSI value goes up. Both indexes indicate that at different penetration levels, the voltage stability of the system deteriorates as the load increases. The *P-V* curve in Figure 8 shows that the load margin of the system increases, and the NVSI value decreases in Figure7 when the PV penetration increases from 0% to 60%. Even though the NVSI index of the weak bus with 60% PV penetration level is a negative value, it can reflect the voltage stability of the power system. The voltage magnitude of this bus is higher than the base case.

4. Conclusion

The PV generation system impact on the power system static voltage stability is analyzed using the NVSI index, I_{LM} index and *P-V* curve with different research scenarios. The analysis results show that integrating PV plants improves the static voltage stability at weak bus within the power system. It also mitigates the voltage drop caused by load increases, enhancing the system load margin. NVSI can effectively represent the voltage stability of the system in any situation. However, at a high PV penetration level, it can also affect the secure and stable operation of the power system. In

summary, the PV generation can enhance the voltage stability of the power system. Nevertheless, it is essential to strategically plan the installed capacity of PV plants to guarantee the system secure and dependable functioning.

Compliance with ethical standards

Acknowledgments

This work was supported by the Postgraduate Research & Practice Innovation Program of Jiangsu Province (SJCX23_1195), and the Graduate Student Innovation Fund of Nanjing Institute of Technology (TB202317052).

Disclosure of conflict of interest

The Authors confirm that the content of this manuscript has no conflict of interest.

References

[1] Zhang H, Yu Z, Zhu C, et al. Green or not? Environmental challenges from photovoltaic technology[J]. Environmental Pollution, 2023: 121066.

[2] ZHAO Jingbo, ZHANG Sicong, LIAO Shiwu. Analysis and thoughts on the mid-August 2020 power outage in California, USA[J]. Power Engineering Technology, 2020, 39(6): 52-57.

[3] YUAN Jinglei, HAN Weiheng, CHENG Qiang. Waveform analysis of two consecutive total stop events in a distributed PV plant[J]. Shanxi Electric Power, 2019(4): 30-34.

[4] QI Jinshan, YAO Liangzhong, LIAO Siyang, et al. Online probabilistic assessment of static voltage stability margin for power systems with a high proportion of renewable energy [J]. Power System Protection and Control, 2023, 51(5): 220677

[5] Jansson P M, Michelfelder R A, Udo V E, et al. Integrating Large-Scale Photovoltaic Power Plants into the Grid[C]//2008 IEEE Energy 2030 Conference. IEEE, 2008: 1-6.

[6] Jalboub M K, Rajamani H S, Abd-Alhameed R A, et al. Weakest bus identification based on modal analysis and singular value decomposition techniques[C]//2010 1st International Conference on Energy, Power and Control (EPC-IQ). IEEE, 2010: 351-356.

[7] Moghavvemi M, Jasmon G B. New method for indicating voltage stability condition in power system[C]//Proc. 3rd International Power Engineering Conference. 1997, 1: 223-227.

[8] Yang C F, Lai G G, Lee C H, et al. Optimal setting of reactive compensation devices with an improved voltage stability index for voltage stability enhancement[J]. International Journal of Electrical Power & Energy Systems, 2012, 37(1): 50-57.

[9] Li S, Ma Y, Zhang C, et al. Static voltage stability prediction for PCCs of new energy power stations in the grid-connected system[J]. Journal of Physics: Conference Series. 2022, 2369(1): 012037.

[10] Ajjarapu V, Christy C. The continuation power flow: a tool for steady state voltage stability analysis[J]. IEEE transactions on Power Systems, 1992, 7(1): 416-423

[11] Flueck A J, Dondeti J R. A new continuation power flow tool for investigating the nonlinear effects of transmission branch parameter variations[J]. IEEE Transactions on Power Systems, 2000, 15(1): 223-227.

[12] R. D. Zimmerman and C. E. Murrillo-Sanchez, Matpower Version 6.0 User's Manual, [online] Available: http://www.pserc.cornell.edu/matpower/matpower.html.

[13] Chandra A, Pradhan A K. Online voltage stability and load margin assessment using wide area measurements[J]. International Journal of Electrical Power & Energy Systems, 2019, 108: 392-401.

[14] Chiang H D, Wang C S, Flueck A J. Look-ahead voltage and load margin contingency selection functions for large-scale power systems[J]. IEEE Transactions on Power Systems, 1997, 12(1): 173-180.